

# Shear wave elastography of the saphenous nerve

Mohamed Abdelmohsen Bedewi, MD, PhD<sup>a,\*</sup>, Ayman A. Elsifey, MD<sup>a</sup>, Mamdouh A. Kotb, MD<sup>b,c</sup>, Abdelmohsen Mohamed Bediwy, MS<sup>d</sup>, Yasmin M. Ahmed, MS<sup>e</sup>, Sherine Mohamed Swify, MD<sup>f</sup>, Ahmed M. Abodonya, MD<sup>g,h</sup>

## Abstract

The purpose of this study is to study sonoelastographic features of the saphenous nerve.

The study included 72 saphenous nerves in 36 healthy subjects. High resolution ultrasound and Shearwave elastography were used to evaluate the saphenous nerve. Cross sectional area (CSA) and stiffness were measured.

The mean CSA of the saphenous nerve was 5.7 mm<sup>2</sup>. The mean shear elastic modulus of the saphenous nerve in the short axis was 29.5 kPa. The mean shear elastic modulus of the saphenous nerve in long axis was 29.9 kPa. The saphenous nerve elastic modulus also showed no correlation with CSA in neither the long axis nor short axis. Positive correlation between elasticity measurements in the long and short axes. Age, height, weight, and BMI showed no correlation with saphenous nerve elastic modulus in short or long axes.

The elastic modulus of the saphenous nerve has been determined in healthy subjects and can serve as a reference for future assessment of the saphenous nerve before different procedures.

**Abbreviations:** BMI = body mass index, CSA = cross sectional area, LA = long axis, SA = short axis, SN = saphenous nerve, SWE = shearwave elastography.

**Keywords:** elastography, nerve, neuropathy saphenous, shear wave, ultrasound

## 1. Introduction

The saphenous nerve is the terminal and longest cutaneous branch of the femoral nerve and is derived from L3 and L4 of the lumbar plexus. The SN is purely sensory and has no motor function. The SN emerges as a posterior division of the femoral nerve at the proximal thigh, and runs medial to the femoral artery inside the adductor canal arising from the tunnel with the descending

genicular artery. It then divides into two branches at the level of the medial femoral condyle, the first one is the infrapatellar branch, and the other one is the sartorial branch, which runs along the tibial border accompanied by the great saphenous vein distal to the knee joint. These branches provide sensory innervation to the medial, posteromedial, anteromedial aspects of the distal thigh until the level of the medial malleolus.<sup>[1–5]</sup>

SN blockade is clinically important in surgical procedures distal to the knee because of its purely sensory nature. Surgeries include meniscectomies, ankle, and foot surgeries, in addition to pain management procedures.<sup>[5]</sup>

The SN can be injured at various locations. Entrapment could occur within the sartorius muscle, between the sartorius and the medial femoral condyle, and within the adductor canal. Risk factors for entrapment include increased body weight, genu varum, and tibial torsion. Isolated saphenous neuralgia is not common. Saphenous neuralgia could present with a variety of symptoms, these include sharp burning pain along the distribution of the SN, hyposthesia, dyesthesia, and hyperalgesia.<sup>[6,7]</sup> The SN and its branches are vulnerable to injury during different surgeries around the knee. Injury of the SN after knee procedures is common. This includes arthroscopic repair of the anterior cruciate ligament, total knee replacement, arthrotomy, meniscectomy, medial arthrotomy, and varicose vein stripping. SN injury could also accompany contusions to the lower limb. Compression of the SN could also occur from pes anserine bursitis, ganglion cysts, or injuries from contact sports.<sup>[4,7]</sup>

Over the last two decades, high-resolution ultrasound was used as a complimentary tool for the diagnosis of different neuromuscular disorders. Advantages of ultrasound include short examination time, availability, cheap price, and lack of ionizing radiation. Ultrasound can measure the size of peripheral nerves by measuring the CSA and can also detect some alteration in the nerve echogenicity.<sup>[8–13]</sup>

Editor: Bernhard Schaller.

The authors have no conflicts of interest to disclose.

The datasets generated during and/or analyzed during the present study are available from the corresponding author on reasonable request.

<sup>a</sup> Department of Internal Medicine, Prince Sattam Bin Abdulaziz university, College of Medicine, <sup>b</sup> Neurology Department, College of Medicine, Prince Sattam Bin Abdulaziz University, Al-Kharj, Kingdom of Saudi Arabia, <sup>c</sup> Neurology Department, Faculty of Medicine, Minia University, Minia, <sup>d</sup> Faculty of Medicine, Alexandria University, Alexandria, <sup>e</sup> Faculty of Medicine, Minia University, Minia, <sup>f</sup> Ministry of Health, Alexandria, Alexandria, <sup>g</sup> Anesthesia and Intensive Care Department, Faculty of Medicine, Al-Azhar University, Cairo, Egypt, <sup>h</sup> Surgery Department, College of Medicine, Prince Sattam Bin Abdulaziz University, Al-Kharj, Kingdom of Saudi Arabia.

\* Correspondence: Mohamed Abdelmohsen Bedewi, Department of Internal Medicine, College of Medicine, Prince Sattam Bin Abdulaziz University, P.O. Box 173, Al-Kharj 11942, Kingdom of Saudi Arabia (e-mail: mohamedbedewi@yahoo.com).

Copyright © 2020 the Author(s). Published by Wolters Kluwer Health, Inc. This is an open access article distributed under the terms of the Creative Commons Attribution-Non Commercial License 4.0 (CCBY-NC), where it is permissible to download, share, remix, transform, and buildup the work provided it is properly cited. The work cannot be used commercially without permission from the journal.

How to cite this article: Bedewi MA, Elsifey AA, Kotb MA, Bediwy AM, Ahmed YM, Swify SM, Abodonya AM. Shear wave elastography of the saphenous nerve. *Medicine* 2020;99:37(e22120).

Received: 27 April 2020 / Received in final form: 19 June 2020 / Accepted: 10 August 2020

<http://dx.doi.org/10.1097/MD.00000000000022120>

Knowledge about the sonographic anatomy is essential for successful nerve blockade, pre- and postoperative analgesia and anesthesia, and this could be well demonstrated by high resolution ultrasound.<sup>[14]</sup> Further detailed morphological anatomy is still important for diagnosis of SN entrapment, neuralgia/neuropathy, and different type of injuries. These histological changes are not detected by conventional ultrasound. Elastography was introduced 30 years back to provide information about tissue elasticity. There are two main types of elastography. The first is strain elastography, where mild probe compression is used to estimate tissue stiffness and displacement. The result is a color scale with qualitative and semi-quantitative estimation of elasticity. The other type is shear wave elastography, where a transducer-induced pulse propagates through different tissues in a transverse manner, and then presented in kilopascals (kPa, Young modulus). SWE is reproducible, less operator-dependent and displays quantitative results. Shear wave elastography is now also used in evaluating the breast, thyroid gland, and liver fibrosis. There is now special interest to use SWE for evaluation of the neuromuscular system.<sup>[15–19]</sup> SWE was recently used for the diagnosis of neuropathies involving the median, tibial, and ulnar nerves.<sup>[20]</sup>

To the best of our knowledge, the use of SWE to study the saphenous nerve was not considered before. We believe that in addition to assistance in the evaluation of saphenous injury, and entrapment, SWE could offer extra information of nerve/tissue elasticity alongside conventional ultrasound, thus improving the visibility of the block needle tip/shaft and decreasing the incidence of unintentional intravascular local anesthetic and intraneural puncture.<sup>[21,22]</sup>

The aim of this work is to study the sonoelastographic features of the saphenous nerve at the popliteal fossa.

## 2. Methods

### 2.1. Participants

Seventy-two saphenous nerves were evaluated in 36 healthy adult subjects. After institutional review board approval, participants of the study were recruited between September 2019 and October 2019, and written consent was obtained. Inclusion criteria included healthy subjects (age range 20–46). Exclusion criteria were: history of peripheral neuropathy, numbness or limb pain, weakness, paresthesia, limb surgery. For each participant, data including sex, age, weight, BMI, and height were recorded. Subjects enrolled in this study were free from any diseases related to neuromuscular system, as indicated by and clinical examination and electrophysiologic methods.

### 2.2. Technique

Ultrasound examinations were performed by using an 18 to 5 MHz linear-array transducer (Aixplorer; Mach 30, AixenProvence, France). A radiologist (M.B, 19 years of experience) performed all examinations, images were reviewed by a radiologist (A.E. 10 years' experience). All the participants were examined with the patient in the supine position, semi-flexed knee, and slight external rotation of the hip. To locate the saphenous nerve, the ultrasound probe was positioned in the middle third of the thigh where the femoral artery was identified at its medial part. The sartorius muscle was then identified as an elliptical structure in the short axis. The saphenous nerve is identified in a subsartorial position as a small hyperechoic structure anterior/anterolateral to the femoral artery. The SN is

the first identified in short axis, and then the cross sectional area (CSA) was measured in  $\text{mm}^2$ . For the SWE measurements, each subject was scanned three times with removal of the probe from the skin between measurements. To increase the reliability of the reported stiffness values, a confidence map was used to mask areas below a specific confidence level. Large amount of gel was used with light touch of the probe to decrease pressure effect on the skin. First, the saphenous nerve was identified in short axis and SWE measurements were taken, then the probe was rotated 90 degrees to acquire longitudinal SWE measurements. In each exam, and after identifying the nerve, the probe was held stationary for 3 to 4 s and a 2 mm diameter region of interest (ROI) circle was placed within the hyperechoic epineurium. After viewing the color map, real time shear wave images were recorded with color coding. Longitudinal and transverse split images of the saphenous nerve were taken. Lower image is gray-scale US scan of the saphenous nerve with superimposed color box borders for SWE map and circular ROI for quantitative measurements on upper image. Quantitative SWE measurements shows display of the mean elasticity (Mean), minimum elasticity (Min), and maximum elasticity (Max) with standard deviation (SD) and values reported in kilopascals, kPa. The spectrum of scale colors range from blue for softer tissues through red for stiffer tissues (Figs. 1 and 2).

### 2.3. Electrophysiologic methods

Nerve conduction studies were performed with Nihon-Cohden-Neuropack device. All studies were performed under standard room temperature of 25°C. Hand temperature was maintained at  $\geq 32^\circ\text{C}$ . Electrodiagnostic studies were performed on both hands and feet in all subjects by an expert neurologist.

### 2.4. Statistical analysis

Statistical analysis was performed using Statistical Package for the Social Sciences (SPSS) version 21 software (SPSS Inc, Chicago, IL). Data were presented as mean  $\pm$  standard deviation (SD) and range. Intra-observer variability was measured using Kohen's Kappa test. Independent sample test was used to assess the differences between mean elasticity of the right and left saphenous nerves. The correlations between the mean elasticity bilaterally and age, weight, height, and BMI were calculated by Pearson correlation coefficient test.

## 3. Results

The study included 72 saphenous nerves in 36 healthy adult subjects (21 females, 15 males), with a mean age of  $33.4 \pm 6.5$  (range 20–46), mean height  $160.7 \text{ cm} \pm 9.9$  (range 149–193), mean weight  $63.9 \text{ kg} \pm 14.4$  (range 45–125), mean BMI  $25.1 \pm 3.5$  (range 19.2–33.6). The mean CSA of the saphenous nerve was  $5.7 \text{ mm}^2$  (range  $2-19 \pm 3.3$ ). The mean shear elastic modulus of the saphenous nerve in the short axis was  $29.5 \text{ kPa}$  (range  $12-47 \pm 8.1$ ). The mean shear elastic modulus of the saphenous nerve in long axis was  $29.9 \text{ kPa}$  (range  $14.9-53.7 \pm 8.7$ ). Table 1 shows the demographic characteristics of study participants. Table 2 shows the CSA and stiffness values of the saphenous nerve. The intra-observer reliability calculations resulted in an overall intra-class correlation coefficient of 0.78. No statistical differences were noted between the right and left sides regarding the CSA ( $P = .852$ ), shear wave elastic modulus of the saphenous nerve in short axis ( $P = .763$ ), and shear wave elastic modulus of the saphenous nerve in the long axis ( $P = .338$ ). The CSA of the

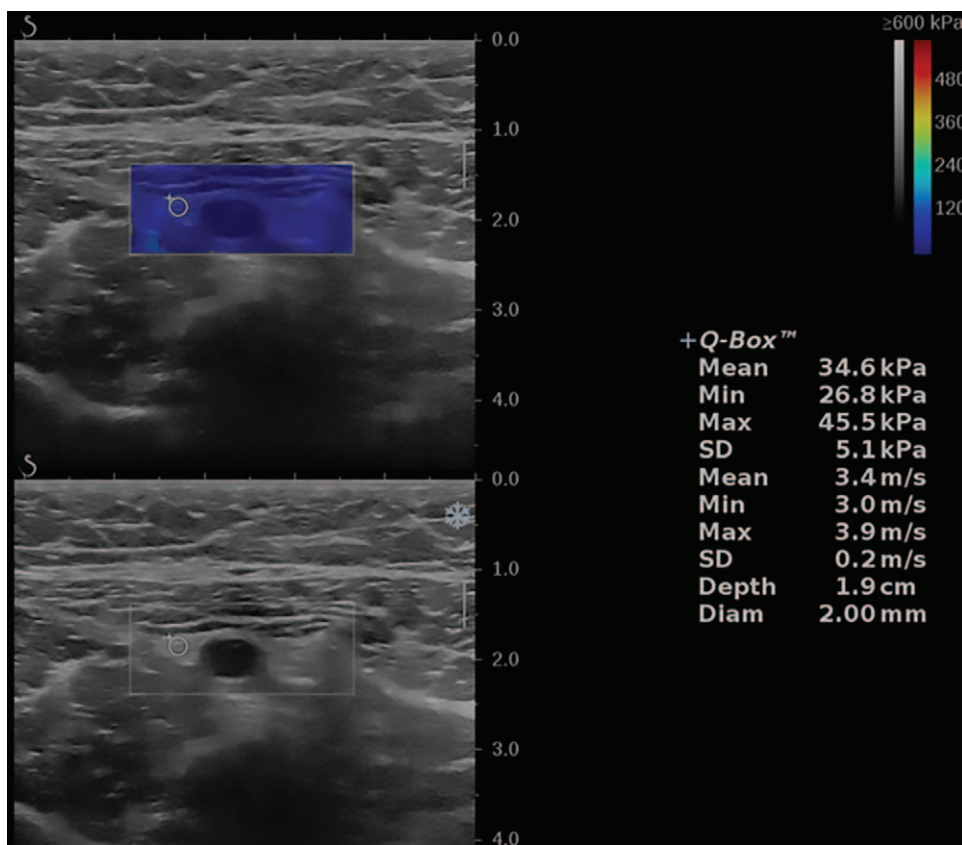


Figure 1. Short-axis view shear wave elastography of the saphenous nerve, with color map, minimum, maximum, and mean stiffness in kPa.

saphenous nerve correlated positively with weight ( $P=.001$ ), BMI ( $P=.002$ ), and height ( $P<.001$ ). No correlation was noted between CSA and age in our study. Positive correlation between elasticity measurements in the long and short axes ( $P<.001$ ). No significant statistical correlation was found between the saphenous nerve elasticity in the long and short axis and the CSA. Age, height, weight, and BMI showed no correlation with the saphenous nerve elastic modulus in short or long axes. Table 3 shows the correlation between the CSA, stiffness, and demographic characteristics in our study.

#### 4. Discussion

We studied the saphenous nerve in healthy adult subjects by SWE. The relationship between elasticity and height, weight, body mass index, gender, were also studied. Some studies

considered elasticity of some peripheral nerves by SWE. Kantraci et al studied the median nerve elasticity by SWE at the level of the carpal tunnel, and revealed a mean stiffness of 32 kPa.<sup>[23]</sup> At the forearm, the median nerve was studied by He et al and showed a mean stiffness of 35 kPa.<sup>[24]</sup> Paluch et al studied the ulnar nerve at two levels, and showed an average stiffness of 33 kPa.<sup>[20,25]</sup> The tibial nerve elasticity was considered in several studies, in most of these studies the tibial nerve ranged between 26 and 36 kPa.<sup>[24,26,27]</sup> The mean stiffness of the saphenous nerve in the our study was (short axis  $29.1 \pm 8.1$  kPa, long axis short axis  $29.9 \pm 8.1$  kPa), was comparable to the elasticity values for the peripheral nerves obtained in other studies. Technical factors are faced when using SWE for assessment of the peripheral nerves. First, is the effect of limb position on SWE, where some postures could lengthen the nerve path resulting in an increase in nerve stretch and subsequent increase in nerve elasticity with such postures.<sup>[28,29]</sup> Second, when the nerve of interest is in close proximity to bone causing unreliable elasticity measurements.<sup>[30]</sup> Third factor was probe orientation, where some authors assessed

**Table 1**  
The demographic characteristics of study participants (mean  $\pm$  standard deviation).

	Mean $\pm$ SD	No %
Age in years	33.4 6.5	
Gender		
Male		15 41.7
Female		21 58.3
Height (cm)	160.7 9.9	
Weight (kg)	63.9 14.4	
Body mass index	25.1 3.5	

SD=standard deviation.

**Table 2**  
CSA and stiffness values of the saphenous nerve (mean  $\pm$  standard deviation).

	Minimum	Maximum	Mean $\pm$ SD
Saphenous CSA	2	19	5.7 3.3
Saphenous SA	12	47	29.5 8.1
Saphenous LA	14.9	53.7	29.9 8.7

CSA=cross sectional area, LA=long axis, SA=short axis, SD=standard deviation.

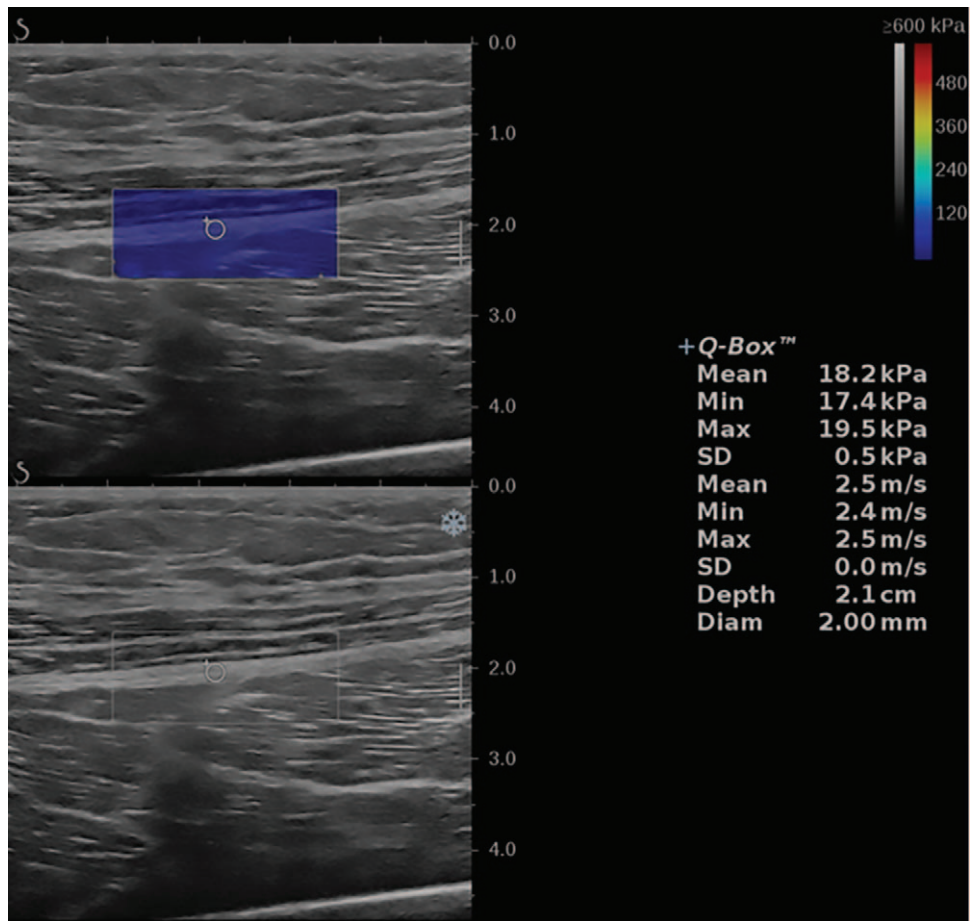


Figure 2. Long axis view shear wave elastography of the saphenous nerve, with color map, minimum, maximum, and mean stiffness in kPa.

Table 3

Correlations between demographic factors, cross sectional area, and stiffness in the long and short axes.

		Saphenous nerve CSA	Saphenous nerve SA	Saphenous nerve LA
Age	Pearson correlation	0.108	-0.099	-0.076
	Sig. (2-tailed)	0.364	0.404	0.523
	N	73	73	73
Height	Pearson correlation	0.605 <sup>†</sup>	0.040	-0.042
	Sig. (2-tailed)	0.000	0.739	0.724
	N	73	73	73
Weight	Pearson correlation	0.666 <sup>†</sup>	-0.046	-0.079
	Sig. (2-tailed)	0.000	0.701	0.506
	N	73	73	73
BMI	Pearson correlation	0.363 <sup>†</sup>	-0.005	-0.012
	Sig. (2-tailed)	0.002	0.969	0.922
	N	69	69	69
Saphenous nerve CSA	Pearson correlation	1	-0.217	-0.175
	Sig. (2-tailed)		0.066	0.139
	N	73	73	73
Saphenous nerve SA	Pearson correlation	-0.217	1	0.443 <sup>†</sup>
	Sig. (2-tailed)	0.066		0.000
	N	73	73	73
Saphenous nerve LA	Pearson correlation	-0.175	0.443 <sup>†</sup>	1
	Sig. (2-tailed)	0.139	0.000	
	N	73	73	73

BMI=body mass index, CSA=cross sectional area, LA=long axis, SA=short axis, SD=standard deviation.

\* Correlation is significant at the 0.05 level (2-tailed).

† Correlation is significant at the 0.01 level (2-tailed).

nerve elasticity in long axis, and others in short axis. In our study, slightly higher values were obtained in the long axis. Long axis elasticity measurements tend to be higher in long axis and is considered more appropriate and reproducible,<sup>[9]</sup> however, examination in the long axis SWE could be challenging in patients with high BMI, and in brachial plexus imaging.<sup>[31]</sup>

Some authors studied the relationship between patient-related characteristics, and biological factors, but the results were inconclusive. Increased depth, thicker superficial fat layers, and greater BMI could be responsible for an attenuation effect that disturbs shear wave collection and create areas of very low/high stiffness in the elastogram.<sup>[32,33]</sup>

This study has some limitations. Small sample size decreases the accuracy of elasticity measurements and limits generalization. Future studies on a large sample size, could help to increase the validity of measurements. In conclusion, we believe that before using the saphenous nerve in different interventional procedures, knowledge of the normal elasticity is necessary.

## Acknowledgments

The authors are grateful to the deanship of scientific research at Prince Sattam bin Abdulaziz University. The authors also would like to thank Dr Mamdouh Kotb for his efforts in the analysis of the biostatistics in this work.

## Author contributions

**Conceptualization:** Mohamed Abdelmohsen Bedewi, Ayman A Elsifey, Mamdouh A Kotb, Abdelmohsen M Bediwy, Yasmin M Ahmed, Sherine M Swify, Ahmed M Abodonya.

**Data curation:** Mohamed Abdelmohsen Bedewi, Mamdouh A Kotb, Sherine M Swify.

**Formal analysis:** Mohamed Abdelmohsen Bedewi.

**Investigation:** Mohamed Abdelmohsen Bedewi, Mamdouh A Kotb.

**Methodology:** Mohamed Abdelmohsen Bedewi, Ayman A Elsifey.

**Project administration:** Mohamed Abdelmohsen Bedewi.

**Resources:** Mohamed Abdelmohsen Bedewi.

**Supervision:** Mohamed Abdelmohsen Bedewi, Ayman A Elsifey.

**Validation:** Mohamed Abdelmohsen Bedewi, Ayman A Elsifey.

**Visualization:** Ayman A Elsifey.

**Writing – original draft:** Mohamed Abdelmohsen Bedewi.

**Writing – review & editing:** Mohamed Abdelmohsen Bedewi.

## References

- [1] Eglitis N, Horn JL, Benninger B, et al. The importance of the saphenous nerve in ankle surgery. *Anesth Analg* 2016;122:1704–6.
- [2] Kent ML, Hackworth RJ, Riffenburgh RH, et al. A comparison of ultrasound-guided and landmark-based approaches to saphenous nerve blockade: a prospective, controlled, blinded, crossover trial. *Anesth Analg* 2013;117:265–70.
- [3] Trescot AM, Brown MN, Karl HW. Infrapatellar saphenous neuralgia—diagnosis and treatment. *Pain Physician* 2013;16:E315–24.
- [4] Chang KV, Mezian K, Naňka O, et al. Ultrasound imaging for the cutaneous nerves of the extremities and relevant entrapment syndromes: from anatomy to clinical implications. *J Clin Med* 2018;7:457.
- [5] Mathew K, Varacallo M. Anatomy, Bony Pelvis and Lower Limb, Saphenous Nerve, Artery, and Vein. *StatPearls* [Internet]. Treasure Island (FL):StatPearls Publishing; Jan 2020–Apr 29, 2019.
- [6] Batistaki C, Saranteas T, Chloros G, et al. Ultrasound-guided saphenous nerve block for saphenous neuralgia after knee surgery: two case reports and review of literature. *Indian J Orthop* 2019;53:208–12.
- [7] Sole JS, Pingree MJ, Spinner RJ, et al. Saphenous neuropathy secondary to extraneural ganglion cyst 15 years after reconstruction of the anterior cruciate ligament. *PM R* 2014;6:451–5.
- [8] Zakrzewski J, Zakrzewska K, Pluta K, et al. Ultrasound elastography in the evaluation of peripheral neuropathies: a systematic review of the literature. *Pol J Radiol* 2019;84:e581–91.
- [9] Wee TC, Simon NG. Ultrasound elastography for the evaluation of peripheral nerves: a systematic review. *Muscle Nerve* 2019;60:501–12.
- [10] Dąbrowska-Thing A, Zakrzewski J, Nowak O, et al. Ultrasound elastography as a potential method to evaluate entrapment neuropathies in elite athletes: a mini-review. *Pol J Radiol* 2019;84:e625–9.
- [11] Winn N, Lalam R, Cassar-Pullicino V. Sonoelastography in the musculoskeletal system: current role and future directions. *World J Radiol* 2016;8:868–79.
- [12] Davis LC, Baumer TG, Bey MJ, et al. Clinical utilization of shear wave elastography in the musculoskeletal system. *Ultrasonography* 2019;38:2–12.
- [13] Klausner AS, Miyamoto H, Bellmann-Weiler R, et al. Sonoelastography: musculoskeletal applications. *Radiology* 2014;272:622–33.
- [14] Ghosh A, Chaudhury S. Morphology of saphenous nerve in cadavers: a guide to saphenous block and surgical interventions. *Anat Cell Biol* 2019;52:262–8.
- [15] Taljanovic MS, Gimber LH, Becker GW, et al. Shear-wave elastography: basic physics and musculoskeletal applications. *Radiographics* 2017;37:855–70.
- [16] Ryu J, Jeong WK. Current status of musculoskeletal application of shear wave elastography. *Ultrasonography* 2017;36:185–97.
- [17] Hobson-Webb LD. Emerging technologies in neuromuscular ultrasound. *Muscle Nerve* 2020;61:719–25.
- [18] Wildeboer RR, Sloun RJGv, Mannaerts CK, et al. Synthetic elastography from B-mode ultrasound through deep learning. 2019 IEEE International Ultrasonics Symposium (IUS), Glasgow, UK, 2019, 108–110.
- [19] Gao Z, Wu S, Liu Z, et al. Learning the implicit strain reconstruction in ultrasound elastography using privileged information. *Med Image Anal* 2019;58:101534.
- [20] Paluch Ł, Noszczyk B, Nitek Ż, et al. Shear-wave elastography: a new potential method to diagnose ulnar neuropathy at the elbow. *Eur Radiol* 2018;28:4932–9.
- [21] Munirama S, Zealley K, Schwab A, et al. Trainee anaesthetist diagnosis of intraneural injection—a study comparing B-mode ultrasound with the fusion of B-mode and elastography in the soft embalmed Thiel cadaver model. *Br J Anaesth* 2016;117:792–800.
- [22] Munirama S, Satapathy AR, Schwab A, et al. Translation of sonoelastography from Thiel cadaver to patients for peripheral nerve blocks. *Anaesthesia* 2012;67:721–8.
- [23] Kantarci F, Ustabasioglu FE, Delil S, et al. Mihmanli Median nerve stiffness measurement by shear wave elastography: a potential sonographic method in the diagnosis of carpal tunnel syndrome. *Eur Radiol* 2014;24:434–40.
- [24] He Y, Xiang X, Zhu BH, et al. Shear wave elastography evaluation of the median and tibial nerve in diabetic peripheral neuropathy. *Quant Imaging Med Surg* 2019;9:273–328.
- [25] Paluch Ł, Noszczyk BH, Walecki J, et al. Shear-wave elastography in the diagnosis of ulnar tunnel syndrome. *J Plast Reconstr Aesthet Surg* 2018;71:1593–9.
- [26] Jiang W, Huang S, Teng H, et al. Diagnostic performance of two-dimensional shear wave elastography for evaluating tibial nerve stiffness in patients with diabetic peripheral neuropathy. *Eur Radiol* 2019;29:2167–74.
- [27] Dikici AS, Ustabasioglu FE, Delil S, et al. Evaluation of the tibial nerve with shear-wave elastography: a potential sonographic method for the diagnosis of diabetic peripheral neuropathy. *Radiology* 2017;282:494–501.
- [28] Greening J, Dilley A. Posture-induced changes in peripheral nerve stiffness measured by ultrasound shear-wave elastography. *Muscle Nerve* 2017;55:213–22.
- [29] Rugel CL, Franz CK, Lee SSM. Influence of limb position on assessment of nerve mechanical properties using shear wave ultrasound elastography. *Muscle Nerve* 2020;61:616–22.
- [30] Bortolotto C, Turpini E, Felisaz P, et al. Median nerve evaluation by shearwave elastosonography: impact of “bone-proximity” hardening artifacts and inter-observer agreement. *J Ultrasound* 2017;20:293–9.
- [31] Aslan A, Aktan A, Aslan M, et al. Shear wave and strain elastographic features of the brachial plexus in healthy adults: reliability of the findings—a pilot study. *J Ultrasound Med* 2018;37:2353–62.
- [32] Creze M, Nordez A, Soubeyrand M, et al. Shear wave sonoelastography of skeletal muscle: basic principles, biomechanical concepts, clinical applications, and future perspectives. *Skeletal Radiol* 2018;47:457–71.
- [33] Ishibashi F, Taniguchi M, Kojima R, et al. Elasticity of the tibial nerve assessed by sonoelastography was reduced before the development of neuropathy and further deterioration associated with the severity of neuropathy in patients with type 2 diabetes. *J Diabetes Investig* 2016;7: 404–12.